Biophysical Journal, Volume 99

Supporting Material

Apparent Tradeoff of Higher Activity in MMP-12 for Enhanced Stability and Flexibility in MMP-3

Xiangyang Liang, Arunima, Yingchu Zhao, Rajagopalan Bhaskaran, Anuradha Shende, Todd S. Byrne, Jeremy Fleeks, Mark O. Palmier, and Steven R. Van Doren

MATERIALS AND METHODS (continued)

Preparation of MMPs

The MMP-12 catalytic domain, with or without the E219A mutation that prevents autolysis, was prepared, labeled with ^{15}N, and dialyzed into 20 mM imidazole, 10 mM $CaCl_2$, and 100 μM $ZnCl_2$ at pH 6.6 for NMR (1), or another buffer for activity measurements (Table 1) (2). Wild type MMP-3 catalytic domain was prepared (3), labeled with ^{15}N, and dialyzed into the same buffers used for MMP-12.

NMR data acquisition

Standard triple resonance spectra were acquired on MMP-3 catalytic domain in order to revise assignments of its backbone amide groups. These and ^{15}N R_1 and R_2 relaxation rates, $^{15}N\{^1H\}$ steady-state NOE, and qualitative relaxation dispersion experiments were acquired at 26 °C on a Varian Inova 600 spectrometer with 5 mm cryogenic probe. ^{15}N R_1 series were also collected on Bruker DMX-500 with 5 mm cryogenic probe (NMRFAM) in order to supply the fourth relaxation measurement needed statistically for fitting three parameters (S^2, R_{ex} and τ_e) in model-free analysis. The series of relaxation spectra used to prepare Fig. 1 were collected on 800 MHz spectrometers at either EMSL (MMP-12(E219A)) or U. of Missouri (MMP-3 catalytic domain). The cryogenic probes provided the sensitivity needed for the dilute samples characterized.

Chemical denaturation

Stability of wild type and E219A-substituted MMP-12 against denaturation by guanidinium chloride (GdmCl) were monitored by intrinsic tryptophan fluorescence using a fluorescence plate reader (4) (Fig. S4). Stock solutions of folded and denatured enzyme (25 μg/ml or 1.3 μM each) in 20 mM Tris·HCl, 5 mM $CaCl_2$, and 20 μM $ZnCl_2$ were mixed and fully equilibrated about 15 min at 25 ºC. Tryptophan fluorescence was excited at 280 nm and detected at 316 nm in rapid succession through the samples on a BioTek Synergy MX plate reader.

RESULTS (continued)

Inquiry into any residual self-association

Prior to intensive NMR relaxation studies, we evaluated the concentration ranges where each protease is monodisperse or subject to self-association. The line broadening was evident in spectra of 0.5 mM MMP-3 catalytic domain and 0.94 mM MMP-12(E219A) (Fig. S1), suggesting self-association at these concentrations. MMP-12(E219A) experiences less self-association with shallower concentration dependence. To avoid line broadening

contributions of self-association to relaxation spectra, we acquired them using 0.15 to 0.28 mM MMP-3 catalytic domain and 0.21 to 0.35 mM MMP-12(E219A).

We investigated the possibility of any residual self-association accounting for exchange broadening observed under dilute conditions in Fig. 1, 2, 3 and of any particular surface of mediating self-association. For the latter, we looked for any concentration-dependent chemical shift perturbations (CSPs). However, CSPs were not observed upon increasing the concentration of MMP-3 catalytic domain to 0.5 mM, other than slight shifts of the amide peaks of T191 and G247 having $\Delta\omega_H$ of 0.009 and 0.013 ppm, respectively. CSPs were also not observed upon increasing concentration of MMP-12(E219A) from 0.35 to 0.94 mM, except for very slight shifts of W203ε1, V235, and K241 (each with $\Delta\omega_H$ = 2 Hz = 0.0033 ppm) and I180 ($\Delta\omega_H$ = 4 Hz = 0.007 ppm). As these four residues lie in loops near the active site, it is possible that the active site could mediate self association at 0.94 mM. However, all four residues lack any exchange broadening at 0.21 mM in the analysis of Fig. 1 that amplifies any such broadening. These observations suggest freedom from artifacts from self-association under the dilute conditions employed for comparing dynamics of the enzymes.

The half of residues that increased in line width (i.e. ≥ 20%) the most as concentration was increased, either to 0.5 mM MMP-3 catalytic domain or to 0.94 mM MMP-12(E219A), proved *not* more likely to have exchange broadening in the spectra of the dilute samples described in Fig. 1, 2, 3 (Table S1). In both MMPs, the half of residues most subject to concentration-dependent line broadening (with R_2 at high concentration at least 20% higher than at low concentration) are less than or equally likely as *all* residues to manifest exchange broadening at low concentrations (Table S1). The residues with the most concentration-dependent broadening are scattered over the entirety of each catalytic domain, without being concentrated around the active site. This contrasts the enrichment of broadening at low concentration in regions around the active site cleft of each MMP (Fig. 1e-h). Thus, it appears quite unlikely that the line broadening of either dilute MMP-12(E219A) or dilute MMP-3 catalytic domain reported in Figs. 1, 2, and 3 are attributable to concentration-dependent self association.

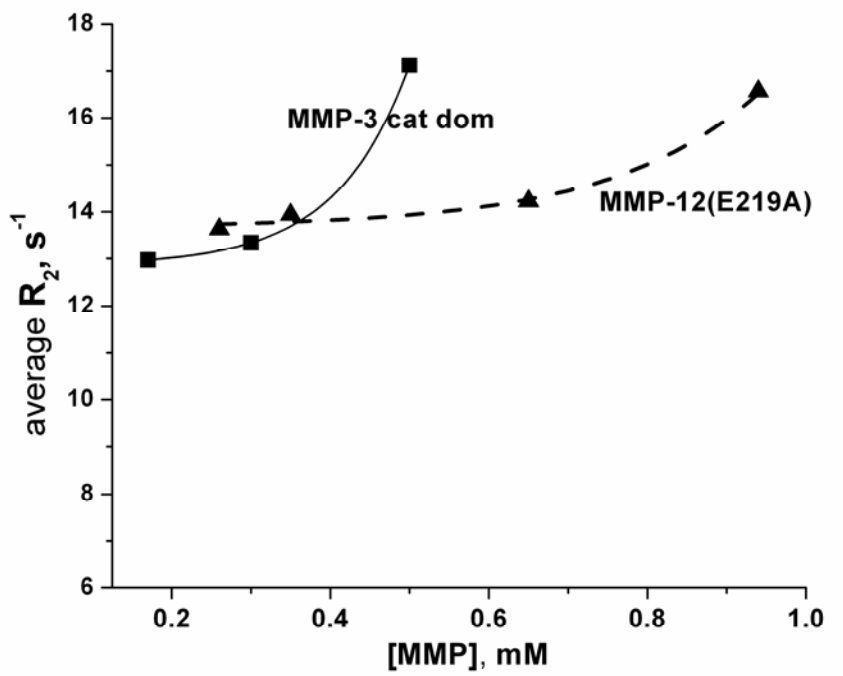

Figure S1. Concentration dependence of spin-spin ^{15}N relaxation rate constants, R_2, of MMP-12(E219A) at 26°C (triangles, averaged over all residues) and MMP-3 catalytic domain at 34°C (squares, averaged over a subset of 30 residues).

Table S1. The fraction of residues with line broadening introduced by elevated concentration is less than or equal to the fraction with line broadening already present at low concentrations.

Samples	Conditions, portion of residues	Exchange broadening observed in: Analysis of Fig. 1	Analysis of Fig. 3
MMP-3 cat dom	Half of residues most broadened by concentration increase to 0.5 mM	54%	51%
MMP-3 cat dom	All residues characterized; ≤ 0.28 mM	56%	59.5%
MMP-12 (E219A)	Half of residues most broadened by concentration increase to 0.94 mM	23.5%	35%
MMP-12 (E219A)	All residues characterized; ≤ 0.35 mM	30%	44%

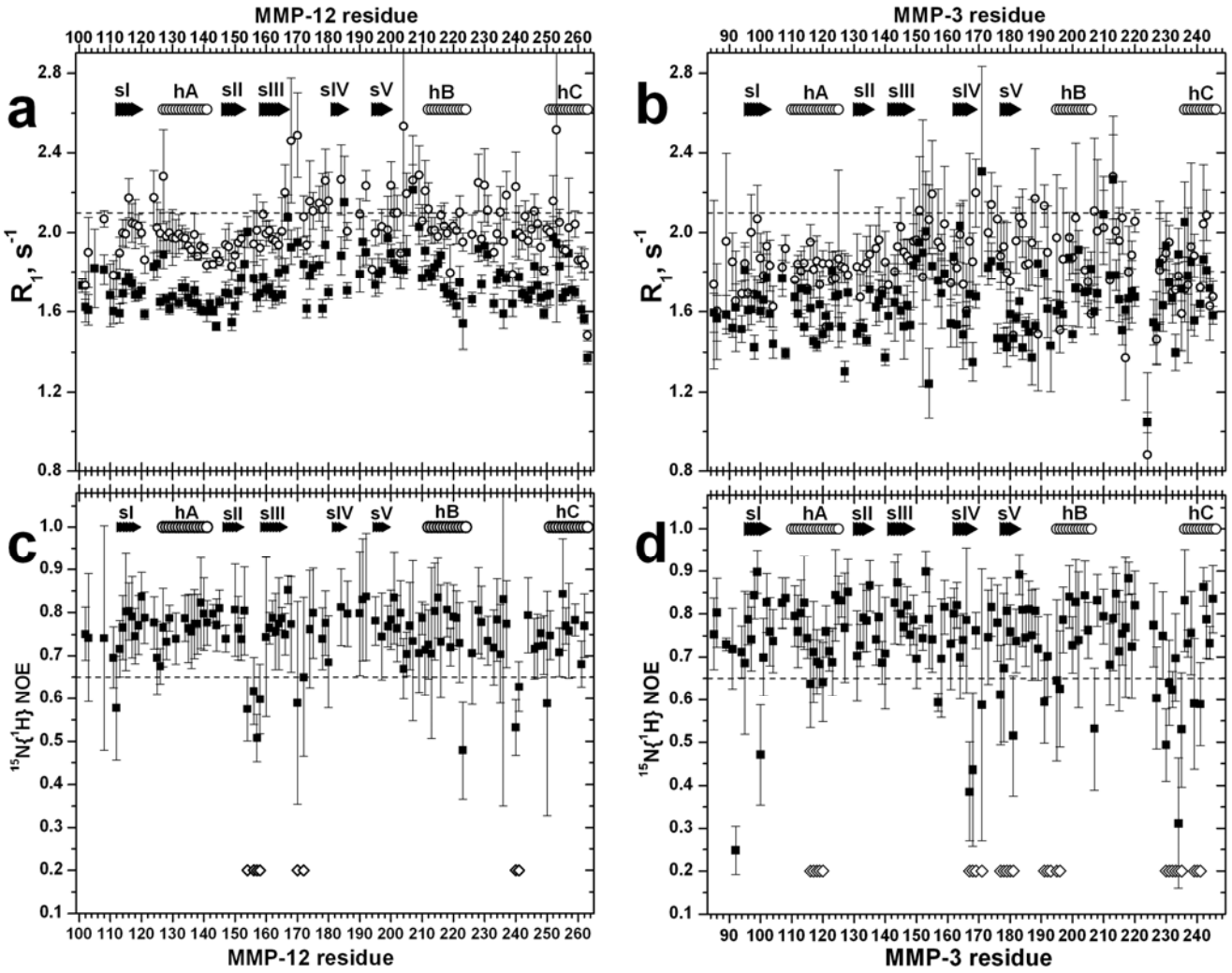

Figure S2. Amide ^{15}N R_1 (upper panels) and $^{15}N\{^1H\}$ NOE (lower panels) relaxation of MMP-12(E219A) (left panels) and MMP-3 catalytic domain (right panels) at 26°C. Spin-lattice relaxation rate constants, R_1 (a, b) were measured at both 11.74 and 14.1 T, represented by open circles and filled squares, respectively. $^{15}N\{^1H\}$ NOE at 14.1 T is plotted as I_{sat} / I_{nonsat} (c, d). Panel c depicts an average of five repetitions and panel d an average of six repetitions. The thresholds designate enrichment of nanosecond fluctuations above the dashed lines in panels a and b and faster fluctuations below the dashed lines in c and d. Secondary structure is marked by arrows for β-strands and cylinders for α-helices. Open diamonds in c and d mark segments with two or more residues enriched in fast fluctuations, in contrast to the homologous enzyme.

Table S2. Average relaxation parameters of the more rigid residues.

	coarse-filtered [1]						fine-filtered [2]				
	field, T	*n*	^{15}N{^{1}H} $\overline{NOE}$	$\overline{R_1}$, s^{-1}	$\overline{R_2}$, s^{-1}	*n*	^{15}N{^{1}H} $\overline{NOE}$	$\overline{R_1}$, s^{-1}	$\overline{R_2}$, s^{-1}	τ_m, ns	$D_\parallel/D_\perp$
MMP-3	14.1	99	0.77	1.64	15.57	37	0.77	1.63	14.42	9.01 [3]	1.16 [3]
	11.74			1.85				1.83			
MMP-12	14.1	96	0.76	1.74	13.76	43	0.76	1.74	13.03	8.66 [4]	0.88 [4]
	11.74			2.02				2.01			

[1] Coarse filtering removed residues with NOE < 0.65 or with $T_2 \le \overline{T_2} + \sigma_{T2}$ unless $T_1 \ge \overline{T_1} + \sigma_{T1}$ (5). The number of residues remaining after filtering is *n*. Only the set of *n* residues were included in the averages of NOE, R_1 and R_2.

[2] Fine filtering removed residues not fit adequately by the simplest spectral density functions featuring only S^2 *or* S^2 *and* τ_e. Residues with exchange broadening suggested by relaxation dispersion at 600 MHz or statistical need for an R_{ex} term in preliminary model-free calculations were removed. Residues suggested to have nsec-scale motions by $J(\varpi_N = 61MHz) \ge \overline{J(\varpi_N)} + \sigma_{J(\varpi N)}$ were also removed.

[3] Estimated by fitting fine-filtered R_1 and R_2 relaxation to PDB coordinates 1cqr. χ^2 of the prolate fit being only 1.8% lower than the oblate fit suggests ambiguity in the choice.

[4] Estimated by fitting fine-filtered R_1 and R_2 relaxation to PDB coordinates 2poj.

Table S3. Counts of residues needing the spectral density functions listed for the Lipari-Szabo model-free approach.

Function	*fit parameters*	*MMP-12(E219A)*	*MMP-3 catalytic domain*
1	S^2	22	26
2	S^2, τ_e	27	21
3	S^2, R_{ex}	23	45
4	S^2, τ_e, R_{ex}	31	33
5	S_s^2, S_f^2, τ_e	0	0

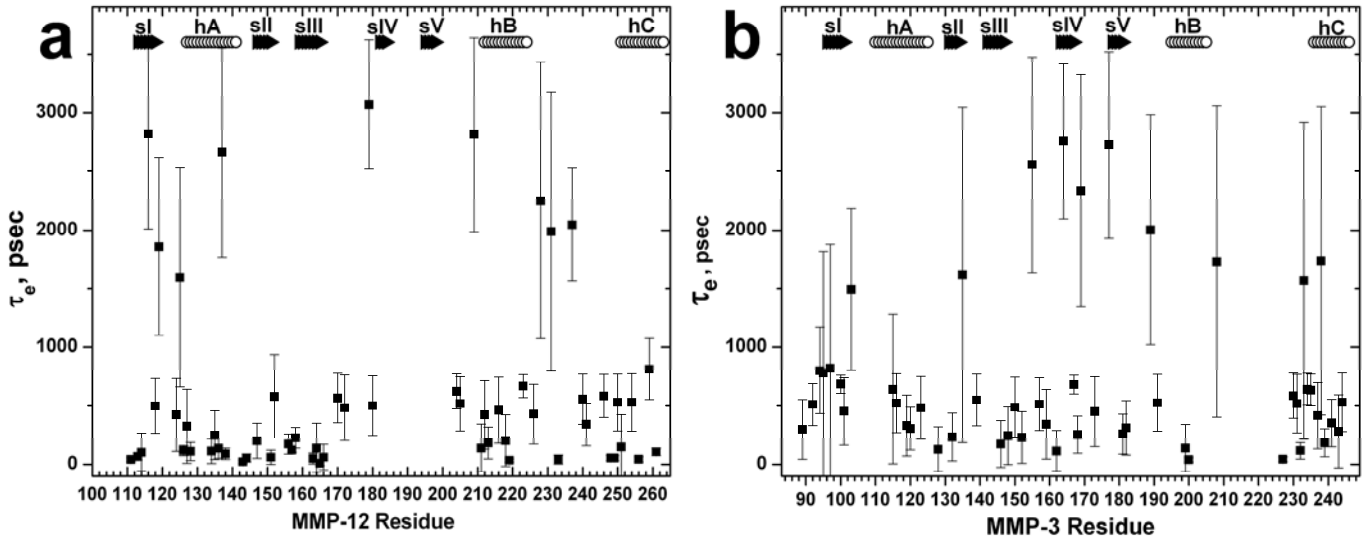

Figure S3. Model-free internal correlation time τ_e (at 26 °C) plotted vs. residue number of (a) MMP-12(E219A) or (b) MMP-3 catalytic domain.

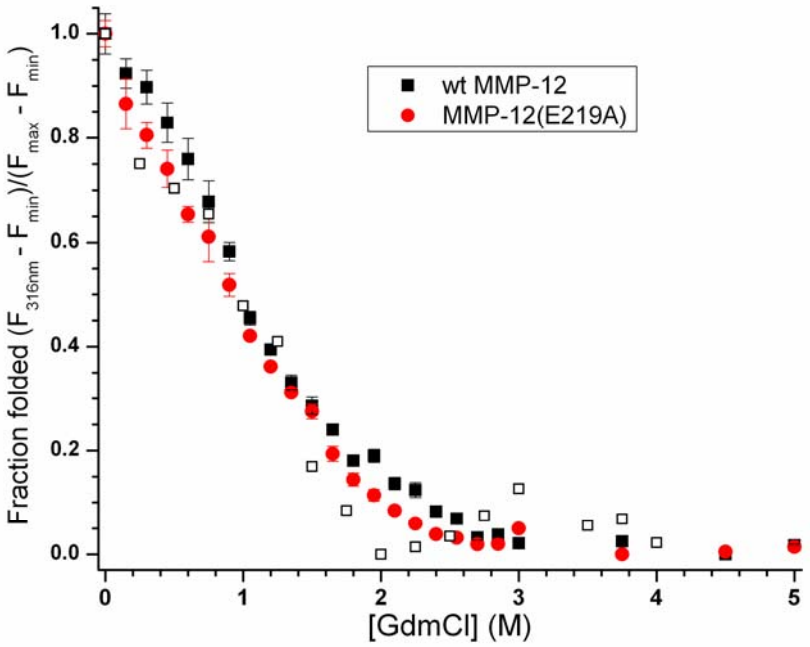

Figure S4. Wild-type and E219A-inactivated MMP-12 are similarly highly sensitive to denaturation by GdmCl. Intrinsic tryptophan fluorescence of the folded state was monitored at 316 nm at 25 ºC with 25 µg/ml (1.3 µM) protein. Solid symbols are averages of triplicate sets of samples. Open squares represent an independent single set of wild type samples, for perspective on experimental uncertainty.

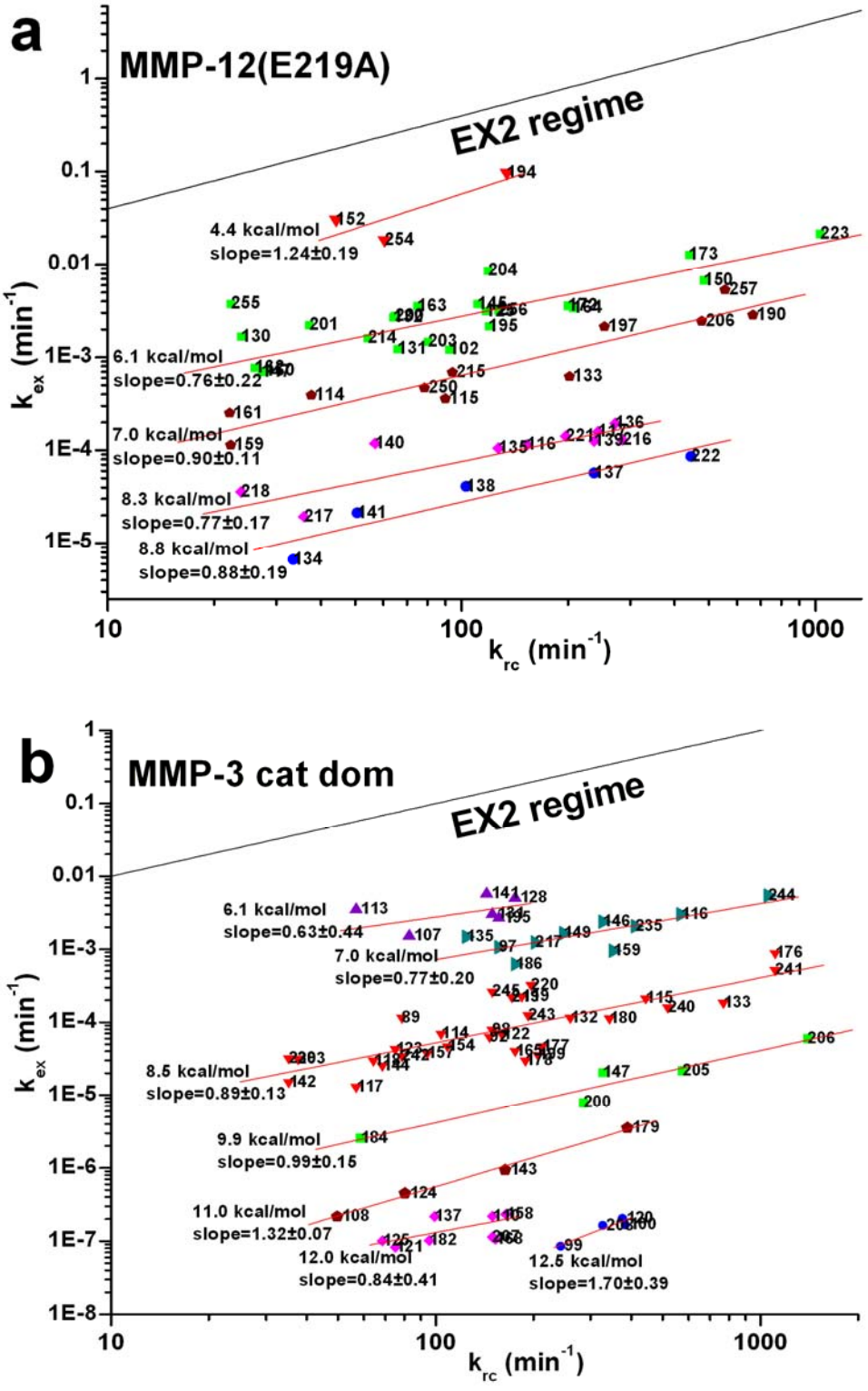

Figure S5. Rates of amide hydrogen exchange of MMP-12(E219A) (a) and MMP-3 catalytic domain (b) support EX2 behavior. Amide groups are clustered into tiers with average apparent ΔG_{HX} , slopes, and residue numbers listed. The reference line depicts the slope of 1.0 typifying the theoretical behavior of the EX2 regime. The symbol colors and types of the tiers match those of Fig. 4a,b that plot ΔG_{HX} vs. residue numbers.

REFERENCES

1. Bhaskaran, R., M. O. Palmier, N. A. Bagegni, X. Liang, and S. R. Van Doren. 2007. Solution structure of inhibitor-free human metalloelastase (MMP-12) indicates an internal conformational adjustment. J Mol Biol 374:1333-1344.
2. Bhaskaran, R., M. O. Palmier, J. L. Lauer-Fields, G. B. Fields, and S. R. Van Doren. 2008. MMP-12 Catalytic Domain Recognizes Triple Helical Peptide Models of Collagen V with Exosites and High Activity. J. Biol. Chem. 283:21779-21788.
3. Ye, Q. Z., L. L. Johnson, D. J. Hupe, and V. Baragi. 1992. Purification and characterization of the human stromelysin catalytic domain expressed in Escherichia coli. Biochemistry 31:11231-11235.
4. Aucamp, J. P., A. M. Cosme, G. J. Lye, and P. A. Dalby. 2005. High-throughput measurement of protein stability in microtiter plates. Biotechnol Bioeng 89:599-607.
5. Pawley, N. H., C. Wang, S. Koide, and L. K. Nicholson. 2001. An improved method for distinguishing between anisotropic tumbling and chemical exchange in analysis of 15N relaxation parameters. J. Biomol. NMR 20:149-165.